Polym. Bull. (2015) 72:1975–2000
DOI 10.1007/s00289-015-1384-6

ORIGINAL PAPER

Effects of blend composition and compatibilization on the melt rheology and phase morphology of binary and ternary PP/PA6/EPDM blends

M. Mehrabi Mazidi[1,2] · **Mir Karim Razavi Aghjeh**[1,2]

Received: 24 January 2015 / Revised: 10 March 2015 / Accepted: 6 April 2015 /
Published online: 12 April 2015

Abstract Ternary blends based on isotactic polypropylene (iPP) modified by polyamide 6 (PA6) and ethylene–propylene–diene terpolymer (EPDM) were prepared and their rheological properties were studied. The total content of dispersed phases was kept fixed at 30 wt%. The goal was to investigate the effect of blend composition and compatibilization process using PP-*g*-MA on the dynamic viscoelastic properties of PP/PA6/EPDM ternary systems. Then, attempts were made to correlate the viscoelastic response of the blends with their morphological texture as examined by SEM technique. Different rheological behaviors were observed depending on the dispersed phase(s) type, concentration and alteration of interfacial interaction between the phases. In the blends containing PA6 phase, compatibilization process led to a significant change in the morphology of the blend with a subsequent change in the viscoelastic properties, especially at low-frequency regions. Rheological analysis revealed a deviation from liquid-like behavior for certain binary and ternary systems which were dependent on the PA6 and EPDM contents and the microstructure of the blends as well. In the case of ternary blends, separated-type morphology was observed in consistent with morphology predicted by spreading coefficient concept. The relationship between the morphology and relaxation process of the individual particles was also discussed.

Keywords Blend · Rheology · Morphology · Compatibilization · Relaxation

✉ Mir Karim Razavi Aghjeh
karimrazavi@sut.ac.ir

[1] Institute of Polymeric Materials, Sahand University of Technology, Sahand New Town, 51335-1996 Tabriz, Iran

[2] Faculty of Polymer Engineering, Sahand University of Technology, Sahand New Town, 51335-1996 Tabriz, Iran

Introduction

The melt blending of two or more polymers can provide easy and efficient way to generate new polymeric materials with novel and targeted properties. Because of negligible entropy and positive enthalpy of mixing, most polymer pairs are immiscible from the thermodynamic point of view [1–4]. As a result, their blending gives materials exhibiting poor interfacial adhesion and, hence, inferior mechanical properties with respect to the parent components. It is well known that the presence of certain polymeric species, usually suitably chosen block or graft copolymers, can improve the compatibility between the phases, resulting in finer phase morphology and better adhesion between the phases of the blends through the reduction of interfacial tension. Consequently, phase morphology would be stabilized by inhibition of droplet coalescence in subsequent manufacturing processes which gives rise to better and stable properties of the final products [5–9].

A typical example of immiscible polymers is the system consisting of polyolefins and polyamides, which are intrinsically different in terms of polarity. Blends of polyamides and polypropylene, when are properly compatibilized, can combine some of the best characteristics of both materials: good chemical resistance, low water sorption, high heat deformation temperature and reduced cost. Functionalized polyolefins, such as maleic anhydride (MA)-grafted polypropylene (PP-*g*-MA), are effective compatibilizers for these blends [10–13]. However, due to poor impact strength of the components in PP/PA blends, the impact toughness of the resulting blends, even the compatibilized blends, will be relatively low. In such cases, high levels of toughness can only be achieved by the addition of an appropriate rubber phase that can play the impact modifier role.

The ternary polymer blends consisted of polypropylene (PP), polyamide (PA6 or PA66) and an elastomer have previously been studied [14–24]. Functionalized rubbers and/or thermoplastic elastomers (particularly maleated rubbers) have frequently been utilized to function as both compatibilizer precursors and toughenners for PP/PA blends [15–24]. Reaction between the maleic anhydrides grafted on the rubber phase with the amine end groups of the nylon leads to formation of graft copolymer which preferentially locates at the interface and improves the interfacial adhesion, and hence dispersion of the PA phase in the PP matrix. These works aimed initially to improve the compatibility between PP and PA, and then to establish the relationship between the morphology, mechanical properties and deformation behavior of such ternary polymer blends.

There are also several reports [25–29] that have studied the phase structure and its correlation with dynamic viscoelastic properties of PP-based ternary systems reinforced with other stiff phases and/or rigid fillers. Therefore, the study and development of blends formed by three or more components have raised the attention of both the industrial and the academic world.

In blends consisting of three or more phases, quite different mixed morphologies can be developed. The whole set of properties of these blends, starting with the rheological behavior during processing, is strongly affected by phase structure of minor phases, which depends on several factors such as interfacial energies,

interfacial interaction between the phases and viscoelastic properties of the components [30–33]. Therefore, it is of prime importance to be able to control such parameters in heterogeneous polymer blends.

The aim of this work was to study on ternary blends composed of PP, as the matrix phase, melt mixed with PA6 and EPDM, as the minor components, from morphological and rheological points of view, and to investigate the effect of blend composition and compatibilization process, using a maleic anhydride-grafted polypropylene (PP-*g*-MA), on these behaviors. In addition, binary blends of the three polymers were studied for comparison. In the future parts of this series the detailed results of mechanical properties, fracture toughness and different deformation behaviors of this multiphase system will be presented which provides significant findings observed in these systems.

Experimental

Materials

Polyamide 6 (PA6, with density of 1.13 g/cm^3 and melting temperature of 223 °C) used in this study was Tecomid NB40 NL E. The isotactic polypropylene (iPP) (MFI = 5.0 g/10 min at 2.16 kg and 230 °C, melting temperature of 165 °C) was obtained from Polynar Petrochemical Co., Tabriz, Iran. Maleic anhydride-grafted polypropylene (PP-*g*-MA; MFI = 80 g/10 min at 2.16 kg and 230 °C, and with 1 wt% grafted MA) as a compatibilizer precursor was obtained from Crompton Corporation. The EPDM used (KEP270) with mass density of 0.96 g/cm^3 and moony viscosity ML(1 + 4) 125 °C:71, supplied from Kumho Polychem, South Korea, was a medium ethylene grade (contents of ethylene, propylene and ethylidene norbornen: 57, 38.5 and 4.5 wt%, respectively).

Blends preparation

To avoid the effect of moisture, all the materials were dried in a vacuum oven at 80 °C for 12 h prior to mixing. All the blends were prepared in an internal mixer (Brabender W50EHT) with a rotor speed of 60 rpm at 230 °C for 8 min. In the case of compatibilized blends, the PP-*g*-MA was added into the mixing chamber at about 3 min from the beginning of the mixing process. The same processing condition was applied for the pure polymeric materials as reference samples. Obtained samples were compression molded into suitable pieces for rheometry analysis. Molding was carried out at 230 °C followed by slow water-cooling under low pressure. A small amount of the prepared blend samples was rapidly quenched in liquid nitrogen for morphological studies.

Morphological observations

A TESCAN FEG scanning electron microscopy (SEM) instrument was used for morphological studies. Cryo-fractured surfaces, in liquid nitrogen, were gold

sputtered for good conductivity of the electron beam and microphotographs were taken within different magnifications. For better understanding of dispersion state of the dispersed phases, a selective extraction was applied to the EPDM phase domains. For this purpose, the EPDM phase was selectively extracted in Cyclohexane solvent at room temperature for 24 h. Then, the samples were dried at 85 °C in a vacuum oven overnight. The size of the dispersed phases was measured using the image analysis software (Image Pro Express). Then, the size distribution of the dispersed components was determined by size measurements of approximately 300 (for PA6 particles) and 700 (for EPDM nodules) domains from sets of cryo-fractured SEM micrographs.

FT-IR analysis

The chemical structures of the blends were characterized using a Fourier transform infrared (FT-IR) spectrophotometer (TENSOR 27). FT-IR analyses were performed on films made of samples.

Rheological studies

The flow behavior and melt linear viscoelastic properties of different samples were investigated using a dynamic rheometer (MCR301, Anton Paar) equipped with a parallel plate geometry (diameter = 25 mm, gap = 1 mm). The strain sweep tests were performed in the range of 0.01–100 % to determine the linear viscoelastic range at 230 °C. Then, the frequency sweep tests were performed in the range of 0.04–625 rad/sat the same temperature under dry nitrogen atmosphere with amplitude of 1 % to maintain the response of materials in the linear viscoelastic region.

Results and discussion

Dynamic rheology

Strain sweep test

Figure 1 shows the storage modulus (G') and loss modulus (G'') as functions of strain for some of blend systems. The results clearly show that the response of the blends lies in the range of linear viscoelastic up to 10 % strain. Based on this finding, the frequency sweep tests were conducted at 1 % strain amplitude to evaluate the response of all the materials in the linear viscoelastic region.

Frequency sweep tests

PP/PA6 binary blends The rheological properties of neat PP and PA6 as well as their binary blends are shown in Fig. 2. It is clear from Fig. 2a that neat polymers exhibit a Newtonian plateau behavior at low-frequency region.

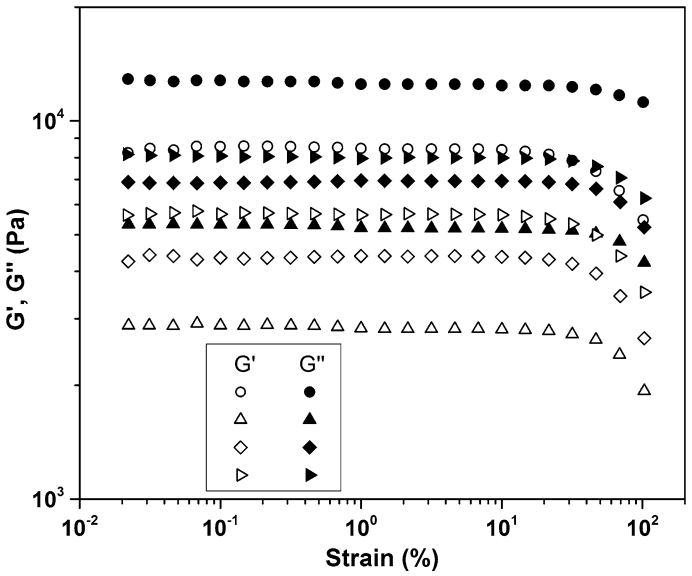

Fig. 1 Strain dependence of storage (G') and loss (G'') moduli for some of blend systems. (*open circle*, *filled circle*) PP/EPDM (70/30), (*open triangle*, *filled triangle*) PP/PA6 (70/30), (*open diamond*, *filled diamond*) PP/EPDM/PA6 (70/15/15), (*open arrow head*, *filled arrow head*) PP/EPDM/PA6/PP-*g*-MA (65/15/15/5)

As depicted in Fig. 2a, incorporation of PA6 into PP resulted in an increase in the complex viscosity (η^*) of the blend. Compatibilization further increased the complex viscosity of PP/PA6 blend over the entire range of frequency. The difference in flow behavior between uncompatibilized and compatibilized blends becomes more pronounced as the angular frequency is reduced. This indicates that the interaction between the PP and PA6 phases significantly increases upon the addition of PP-*g*-MA, which acts as a compatibilizer precursor. It is known that during the melt mixing process, the maleic anhydride groups of PP-*g*-MA chemically react with the amine end groups and/or amid linkages of the PA6 chains leading to the formation of PA-*g*-PP copolymer at the interfacial region, which strongly enhances the interfacial interaction between the phases. Addition of 30 wt% PA6 into the PP phase increased the storage modulus of the binary system over the entire range of frequency as compared to the pure components. This increased elasticity was more obvious at low frequencies. This type of behavior has already been reported by different researchers for other polymer blends [23, 29]. The increase of elasticity for uncompatibilized PP/PA6 blend at low-frequency ranges could be attributed to the shape relaxation of the dispersed droplets of PA6 minor phase. For compatibilized blend, a shoulder appears and the storage modulus shows a non-terminal trend at low frequencies. It is clearly visible that the elasticity of the compatibilized blend is greater than that of uncompatibilized blend. This suggests that the chain mobility and molecular relaxation processes of the dispersed droplets in the compatibilized blend are severely prohibited, most probably due to

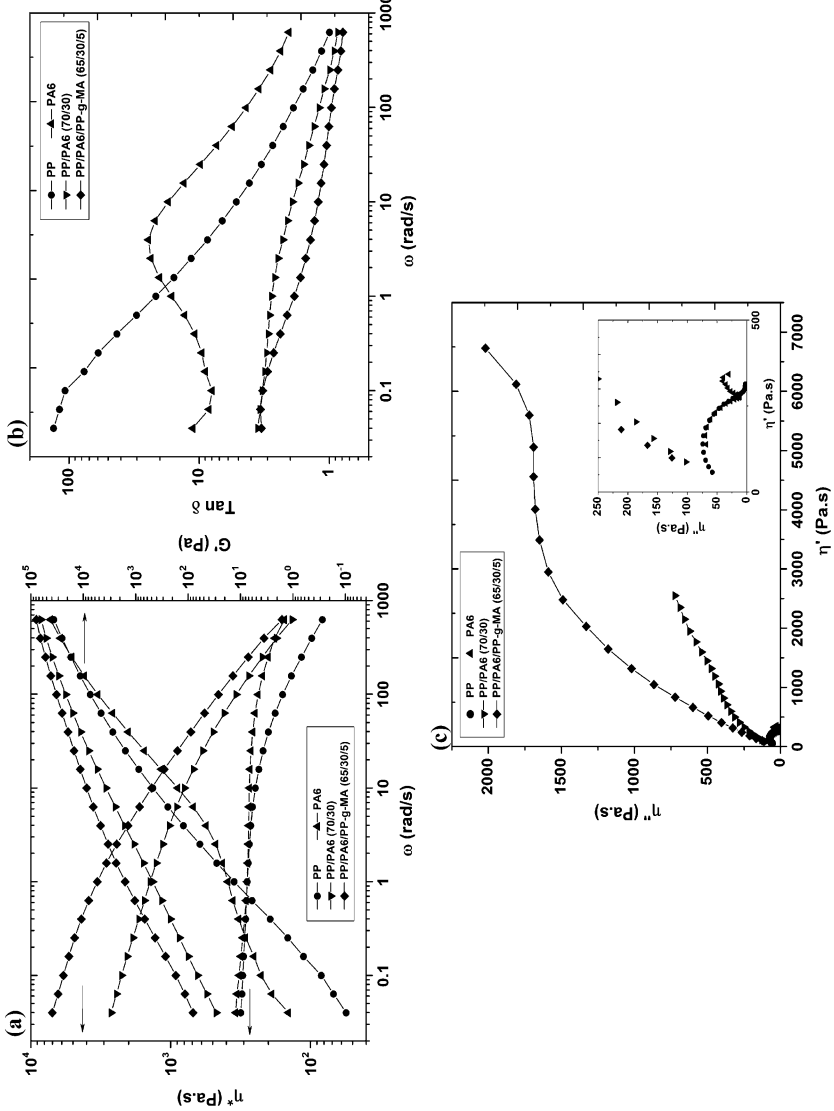

Fig. 2 The rheological properties of pure PP, PA6 and their binary blends at 230 °C. Frequency dependence of **a** complex viscosity and storage modulus, and **b** loss tangent (tan δ). **c** Cole–Cole (η'' vs. η') diagrams

the formation of PA-*g*-PP copolymer. It is noted that increased molecular weight resulting from copolymer formation in the compatibilized blend gives rise to higher complex viscosity and melt elasticity at high-frequency regions compared to those of uncompatibilized binary blend.

A monotonic decrease was observed for damping factor (tan δ) of pure PP as the frequency is increased (Fig. 2b). For PA6, the loss tangent goes through a maximum owing to the molecular structure of PA6 in the molten state. The damping capacity of PP/PA6 binary blends, with and without compatibilizer, is much lower than that of pure components. The decreased damping capability of uncompatibilized PP/PA6 blend compared to the components, especially at low frequencies, arises from the high interfacial tension and, consequently, large shape relaxation of dispersed phase, which is consistent with the melt elasticity of this system as described in Fig. 2a. In the case of compatibilized blend, a poor damping peak can be observed at low frequencies and the relaxation potential of the material is further decreased compared to the uncompatibilized blend. This originates from the greater interactions at the interface region in the compatibilized blend. It is well documented that the relationship between dynamic viscosity ($\eta' = G''/\omega'$ representing the viscous part) and imaginary viscosity ($\eta'' = G'/\omega'$ representing the elastic part), namely the Cole–Cole diagram, reveals the existence of various groups of relaxation times and gives detailed information on the relaxation processes for the polymer blends and filled systems [29, 34–36]. Figure 2c displays the Cole–Cole diagrams of PP, PA6, uncompatibilized and compatibilized PP/PA6 (70/30) blends. High-frequency data are separately represented in the same figure for better observations. In this representation, the frequency regions are clearly separated; at high frequencies the elastic behavior of the blend is dominated by the elasticity of the phases, whereas at low frequencies the effect of the interfacial tension becomes predominant.

The Cole–Cole diagram of pure PP is in the form of a circular arc, characteristic of a homogeneous single-phase system. For pure PA6, a semicircular arc followed by a tail was observed. The observation of relatively broad arc for PP as well as appearance of a tail for PA6 phase may partly be due to the broad molecular weight distribution of these phases. The introduction of PA6 into PP matrix led to a deviation in the shape of the diagram from circular arc to semicircular followed by a tail. This implies that the relaxation behavior of the uncompatibilized PP/PA6 blend shows an additional relaxation process extended toward the lower frequencies corresponding to the longer relaxation times. It is believed that this prolonged relaxation phenomenon is associated with the shape relaxation of the dispersed droplets which imposes a higher elasticity to the binary blend. The addition of PP-*g*-MA caused a dramatic increase in the intensity and frequency range of the relaxation processes of PP/PA6 blend. For compatibilized blend, an intense peak followed by a tail at frequencies much lower than that of uncompatibilized blend is obvious, reflecting that the compatibilization drastically extends the relaxation behavior toward much longer timescales. The origin of this relaxation behavior will further be discussed in the following sections.

PP/EPDM binary blends The rheological characteristics of neat PP and PP/EPDM binary blends are shown in Fig. 3.

It can be seen that the complex viscosity of PP/EPDM blend is higher than that of pure PP particularly at low-frequency ranges. In fact, the incorporation of 30 wt% of EPDM not only suppresses the Newtonian behavior of the pure PP, but also leads to a drastic viscosity upturn in the flow behavior of the material at low-frequency regions. The results also illustrate that the presence of EPDM rubber in the PP phase causes a significant increase in elasticity of the material so that the binary blend showed a non-terminal response at low-frequency regions (Fig. 3a). This phenomenon in dynamic viscoelastic functions, which may be called a "second plateau", is thought to give important information concerning the microstructure of polymeric multicomponent systems. Generally, appearance of a second plateau in the terminal region is considered to be induced by the formation of some kind of ordered structures, for example, an aggregated/agglomerated structure, a skeleton or a network structure in heterogeneous systems [29, 37]. In the PP/EPDM blend, it is believed that development of a network-like structure can be due to the presence of relatively large volume of dispersed EPDM rubber domains with high elasticity and adequate compatibility with the PP matrix. As a result, not only the elasticity and flow resistance of the material have enhanced but also the relaxation processes of the dispersed rubbery particles and their interfaces with the surrounding matrix after shear deformations have been restricted. Moreover, it is observed that addition of PP-*g*-MA has no clear effect on the melt viscosity and elasticity of the PP/EPDM blend, probably due to the lack of a considerable interaction between PP-*g*-MA and EPDM. This finding was further evidenced in the following sections by FT-IR analysis. The damping factor of PP/EPDM shows a great reduction compared to neat PP (Fig. 3b). In addition, a damping peak is apparent for PP/EPDM binary blends. Here, the drastic reduction in loss factor at low-frequency ranges followed by the formation of an intense damping peak for PP/EPDM blends with and without PP-*g*-MA is characteristic of a solid-like behavior. The decrease in tan δ values in PP/EPDM (70/30) blends is an indicator of reduced energy dissipation. In other words, EPDM phase with high melt elasticity retards the relaxation process of chain segments and weakens the inner loss of the blend, and therefore, damping factor decreases in the presence of EPDM. From Fig. 3c, it can be seen that the melt blending of EPDM with PP phase results in a drift in the shape of Cole–Cole diagram from circular shape (pure PP) to linear shape (PP/EPDM blends). It is worth noting that the drastic increase in intensity and frequency range of relaxation behavior results from enhanced elasticity due to the addition of 30 wt% highly elastic EPDM phase followed by the development of more heterogeneous microstructure. In other words, the appearance of a clear shift in Cole–Cole diagrams is an indicator of a higher immiscibility and phase segregation at relatively large volume fraction of EPDM phase, which gives rise to higher heterogeneity of the system.

The rheological data presented above reveal that the PP-*g*-MA has no drastic effect on the linear viscoelastic properties of the PP/EPDM blends, while a different scenario was observed in the case of PP/PA6 blends. Therefore, it can be predicted

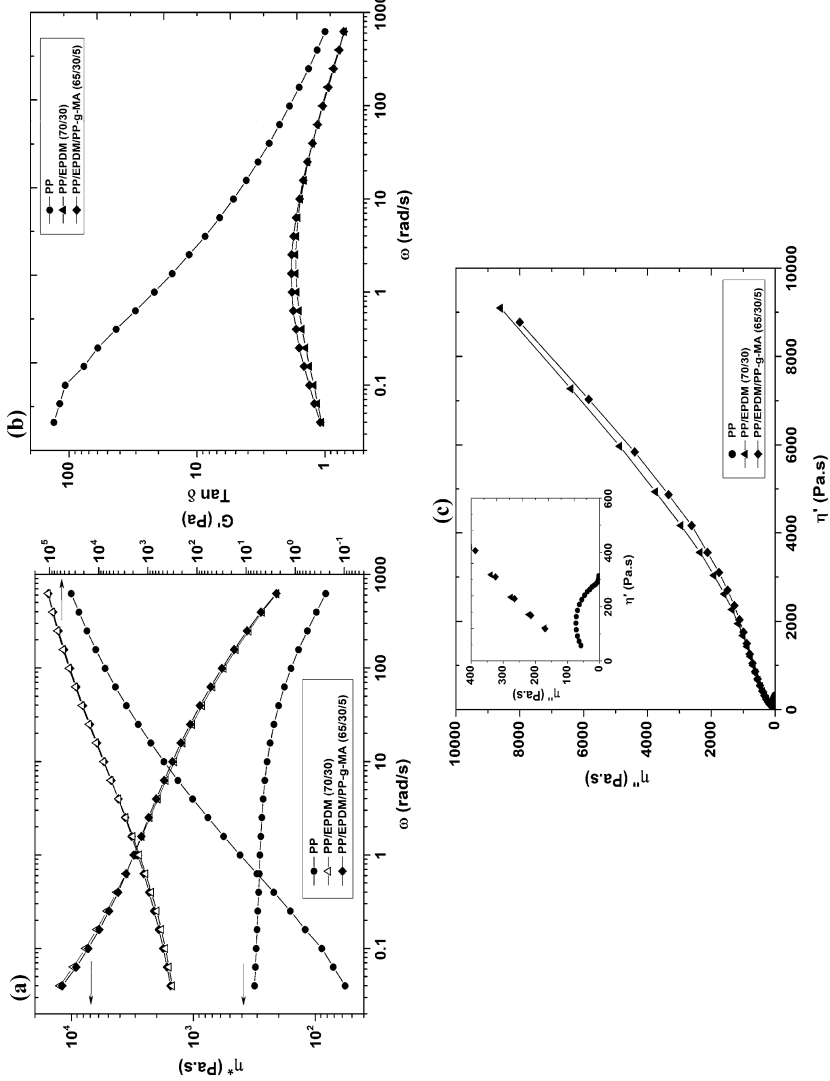

Fig. 3 The rheological properties of neat PP and PP/EPDM binary blends at 230 °C. Frequency dependence of **a** complex viscosity and storage modulus, and **b** loss tangent (tan δ). **c** Cole–Cole (η'' vs. η') diagrams

that in ternary PP/EPDM/PA6 blends, the PP-*g*-MA will preferentially affect PP/PA6 interface and not PP/EPDM interface.

PP/EPDM/PA6 ternary blends This section presents the effects of blend composition and compatibilization, using PP-*g*-MA, on the dynamic viscoelastic properties of PP/EPDM/PA6 ternary systems containing 30 wt% dispersed phase(s). Figure 4 shows different rheological properties of uncompatibilized and compatibilized PP/EPDM/PA6 ternary blends.

From Fig. 4a it is obvious that the complex viscosity of uncompatibilized ternary blends gradually increases with the concentration of EPDM rubbery phase in the dispersed components, so that for the ternary system containing 20 wt% of the EPDM phase an upturn appears at low-frequency regions. This indicates that an increase in the weight fraction of EPDM component from 15 to 20 wt% is accompanied by a change in the phase structure of ternary blend which shows the melt viscosity behavior typical for systems having network-like microstructure. The complex viscosities of compatibilized ternary blends are higher than those of corresponding uncompatibilized blends, and the extent of this increase is determined by the weight fraction of PA6 phase. In other words, the amount of increase in viscosity upon the addition of PP-*g*-MA is greater for the blends of higher PA6 weight fraction. The rheological results presented in previous sections (binary blends) revealed that the PP-*g*-MA greatly affects the viscoelastic properties of PP/PA6 blend, while no effect was observed in the case of PP/EPDM blend. Therefore, chemical affinity of PP-*g*-MA toward PA6 phase and consequently its reaction with PA6 controls the extent of interfacial interactions and the flow characteristics of PP/EPDM/PA6 ternary blends. As a result, as the concentration of PA6 phase in the minor components increases, the change in dynamic viscoelastic properties upon the compatibilization would be larger and vice versa. It is important to note that in Fig. 4a, there is an upturn in the behavior of all the compatibilized ternary systems at low-frequency regions. This suggests that there are strong interfacial interactions and high degree of macromolecular interdiffusions across the interface between the phases in these blends. As outlined above, this type of behavior is characteristic of multiphase systems with solid-like behavior. In the case of storage modulus for uncompatibilized blends, the storage moduli of the blends increase as the concentration of EPDM phase increases. A significant jump in melt elasticity upon increasing of EPDM content from 15 to 20 wt% is clearly visible, so that the blend with 20 wt% of EPDM phase exhibited a shoulder with non-terminal response at low frequencies. The results also demonstrate that elastic modulus of compatibilized blends is greater than that of corresponding uncompatibilized blends, and similar to melt viscosity, the amount of enhancement is directly related to the fraction of PA6 phase. A shoulder appears in the elastic response of all the compatibilized ternary systems similar to uncompatibilized PP/EPDM/PA6 (70/20/10) blend at low-frequency regions, which corresponds with the upturn observed in the complex viscosity curves of the same compositions. It is believed that the frequency, at which the shoulder appears, is associated with the onset of the relaxation of the shape of dispersed domains in the multiphase blends. Although the

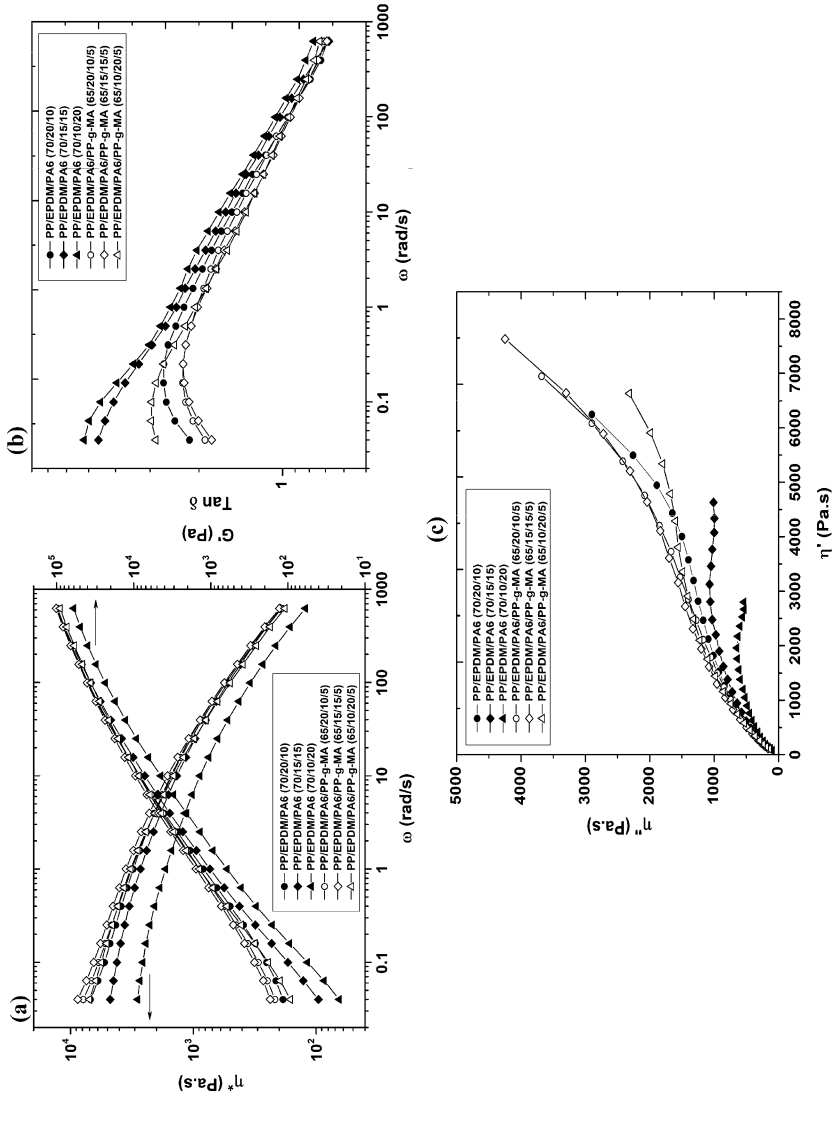

Fig. 4 The rheological properties of uncompatibilized and compatibilized PP/EPDM/PA6 ternary blends of different dispersed phase compositions at 230 °C. Frequency dependence of **a** complex viscosity and storage modulus, and **b** loss tangent (tan δ). **c** Cole–Cole (η'' vs. η') diagrams

uncompatibilized PP/EPDM/PA6 (70/20/10) blend as well as all the compatibilized ternary blends show similarities in their rheological behavior (i.e. deviation from liquid-like behavior), it seems that the origin of this type of behavior for uncompatibilized blend differs from that for compatibilized ones. For uncompatibilized ternary blend with 20 wt% of EPDM phase, appearance of non-terminal behavior at low frequencies mainly originates from the increased phase heterogeneity and larger interfacial areas in the blend as the EPDM phase content increases, so that probably the microstructure progressively transferred from discrete dispersion of EPDM minor component to a percolated EPDM phase particles in the material. Therefore, the increased phase continuity of EPDM phase with much higher elasticity than the other components could be responsible for higher deviation from a liquid-like behavior. Contrary to this, for compatibilized ternary blends the observation of non-terminal behavior at low frequencies primarily arises from increased phase homogeneity of the blend caused by much finer dispersion state of the dispersed components (mainly PA6 phase) in the multiphase system. The compatibilization process promoted by PP-*g*-PA6 copolymer leads to a highly interdiffused macromolecular mixing at the interfacial region between PA6 and PP matrix, producing intimately interlocked phase morphology of the resulting blend. As a result, the chain relaxation and dissipation processes involved in the multiphase compatibilized system become severely inhibited and the blend behaves in a solid-like manner.

It can also be seen in Fig. 4b that the blend composition and/or compatibilization mainly affects the damping behavior at low-frequency regions where the response of materials is mainly determined by the microstructure and interfacial tension between the components. It is clearly visible that for uncompatibilized blends, the loss tangent gradually decreases at low frequencies as the proportion of EPDM in the blend was increased. This reduction in inner loss of the material is more pronounced for the blend of highest amount of EPDM phase, PP/EPDM/PA6 (70/20/10), so that a damping peak is appeared in the loss tangent curve of this ternary blend. For other two uncompatibilized blends, a uniform decrease in damping values was detected as the frequency was increased. Generally, the drastic reduction in loss factor at low-frequency ranges followed by the formation of damping peak in the multiphase polymeric systems is a characteristic of a solid-like behavior resulting from a network-like microstructure [29]. It is believed that higher concentration of EPDM rubbery domains with high melt elasticity and good interfacial adhesion with the PP matrix developed a more heterogeneous network-like microstructure within the matrix which is responsible for a great reduction of damping factor followed by the formation of a damping peak for uncompatibilized blend with 20 wt% of EPDM phase. The compatibilization changes the energy dissipation capacity of the ternary systems especially at low frequencies. The dissipation capability of the compatibilized blends at low frequencies is significantly lower than that of uncompatibilized blends. Moreover, a damping peak appears in the response of compatibilized blends and it seems that this peak intensifies and shifts to higher frequencies as the weight fraction of EPDM in the blend increases. Furthermore, it seems that compatibilization also induces to some extent the network-like response in the ternary systems, especially for blends with higher

loadings of PA6 phase. In this case, the PA-*g*-PP copolymer formed during the melt mixing dramatically promotes the dispersion state of PA6 domains within PP matrix through lowering the interfacial tension and strengthening the interfacial adhesion. Therefore, an intimate mixing state would be achieved through compatibilization.

Further information considering the effects of blend composition and compatibilization on the relaxation behavior of the samples was provided by analyzing the Cole–Cole diagrams, as depicted in Fig. 4c. As can be seen, the shape of Cole–Cole curves gradually deviates from arc-shape to linear-shape as the content of EPDM was increased in the uncompatibilized ternary blends. The increase in weight fraction of EPDM phase from 10 to 15 wt% in uncompatibilized blends causes an increase in the elasticity of the blend and the extension of relaxation behavior of the material toward longer relaxation times. Further increase in the concentration of EPDM rubbery phase from 15 to 20 wt% resulted in a significant upturn in the melt elasticity along with prolonged relaxation response of the sample. The compatibilization remarkably increased the elastic behavior of the samples so that the compatibilized blends have much longer relaxation responses than those of uncompatibilized blends. Moreover, all the compatibilized blends exhibit nearly linear Cole–Cole curves with very high melt elasticity corresponding to the non-terminal response at prolonged relaxation times. It is worth noting that appearance of a linear Cole–Cole response with extensive upturns at very long relaxation times is characteristic of an interconnected microstructure which resembles a solid-like material without terminal zone relaxation. In the multiphase heterogeneous systems, the interconnected phase morphology may arise from a very fine and uniform distribution of the phases within the matrix which leads to a high degree of mixing state and interfacial area interactions as a result of strong intermolecular interactions between different components.

The results of rheological studies revealed that the viscoelastic behavior of uncompatibilized PP/EPDM/PA6 (70/20/10) ternary blend as well as all the compatibilized ternary blends resembles the typical behavior of solid-like materials or the materials with network microstructure. As stated before, the gradual change in relaxation response of the uncompatibilized ternary blends with the proportion of EPDM rubbery phase in the blend could be attributed to the gradual development in phase continuity of EPDM phase with very high melt elasticity in the multiphase system which resembles a network-like microstructure in the ternary blend with the composition of PP/EPDM/PA6 (70/20/10). On the other hand, in the case of compatibilized ternary blends, the increase in molecular weight as well as highly interconnected phase morphology for PA6 phase and PP matrix upon compatibilization strongly impedes the macromolecular relaxation phenomena in the blend, causing a large deviation in liquid-like behavior of the multiphase systems.

Figure 5 shows the relaxation spectrum of binary and ternary blends along with the effect of compatibilization on their relaxation behavior.

According to Fig. 5a, the PP and PA6 spectrums showed single broad peak originated from their molecular weight distribution. However, a low-intensity peak at higher relaxation times can be detected in PA6 spectrum, which seems to be due to the effect of hydrogen bonding between the PA6 chains. The uncompatibilized PP/PA6 binary blend shows a relaxation peak around the relaxation times of PP and

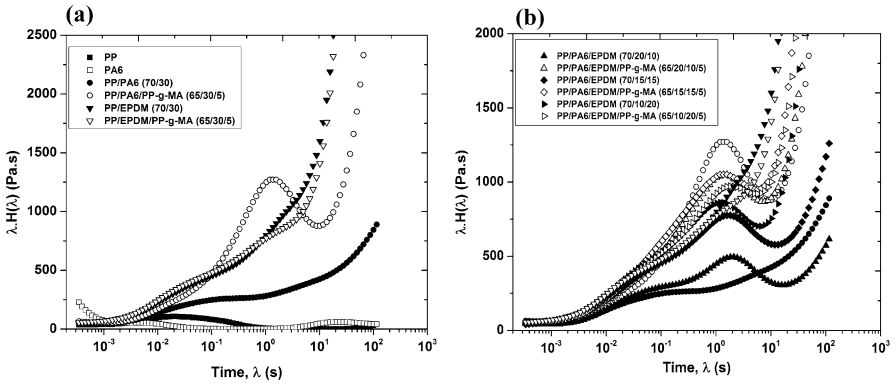

Fig. 5 Weighted relaxation spectrum of different samples. **a** Neat components and binary blends, and **b** uncompatibilized and compatibilized ternary blends of different dispersed phase compositions

PA6 chains followed by a shoulder related to the form relaxation of dispersed PA6 domains in the matrix. In the uncompatibilized PP/PA6 blend this is expected to be the terminal relaxation time of the system. The weighted spectrum of compatibilized PP/PA6 blend exhibits two relaxation peaks followed by the relaxation of the interface. The first shoulder-like peak is related to the relaxation behavior of the blend components. The second strong relaxation peak at longer times can be attributed to the relaxation of the shape of finely dispersed PA6 nodules when sheared. It should be noted that the in situ formation of PP-*g*-PA copolymer at interface increases the interaction between the phases which can further affect the relaxation behavior of the blend. Therefore, the upturn observed in the relaxation behavior of compatibilized PP/PA6 blend is an indication of the presence of an additional relaxation time most probably due to the relaxation of compatibilizer chains at the interfacial region, i.e. interfacial relaxation. This is consistent with the literature that in the compatibilized binary blends the characteristic time for the relaxation of the form of dispersed domains is no longer the terminal relaxation time but the relaxation due to the migration of the compatibilizer chains at the interface happened at much longer time scales is the terminal relaxation process [38, 39]. Similar to compatibilized PP/PA6 blend, the relaxation spectrum of PP/EPDM blend is composed of two relaxation peaks corresponding to relaxation of the components and the shape relaxation of EPDM-dispersed particles together with a prolonged relaxation behavior in the form of an early upturn associated with the interfacial relaxation between the components. This shows that PP/EPDM blend has high compatibility which increases the interface amount and the relaxation times of the chains located at and near the interface. It is also apparent in this figure that the PP-*g*-MA has negligible effect on the relaxation behavior of PP/EPDM blend as resulted earlier using other viscoelastic parameters.

In the case of PP/PA6/EPDM (70/20/10) ternary blend (Fig. 5b), also three different relaxation stages are clearly visible. The first broad peak is due to the relaxation of macromolecular chains of blend components whereas the relaxation

peak at intermediate times may be ascribed to the form relaxation of dispersed PA6 and EPDM droplets in the matrix. The longest relaxation phenomenon could be assigned to the relaxation of the interface between the minor components and the matrix. By considering the fact that the EPDM component is compatible with the surrounding matrix material, it can be concluded that the interfacial relaxation in uncompatibilized PP/PA6/EPDM (70/20/10) system is mainly contributed by the interfacial region between the EPDM-dispersed particles, rather than PA6-dispersed domains, with the PP matrix. It seems that the progressive replacement of PA6 by EPDM phase in the uncompatibilized ternary blends mainly affects the relaxation behavior of the multiphase systems at intermediate and long timescales. The peak related to the relaxation of the form of minor components intensifies and shifts a little back while that for the relaxation of the interface happened at shorter times with higher intensity. In the uncompatibilized ternary blends, this is due to compatibility of highly elastic EPDM component with the PP matrix. Compatibilization of ternary blends further amplifies these relaxation phenomena in the form of an increase in the intensity of shape relaxation (second peak) and earlier upturns observed at the longest relaxation processes (interfacial relaxation). It seems that upon compatibilization, the characteristic time of shape relaxation shifts a little back to shorter times (smaller particles) followed by an earlier and much stronger upturn corresponding to the interface relaxation. These changes in relaxation response of the ternary blends after the addition of compatibilizer precursor mainly originate from the change in the shape- and interface-relaxation processes of PA6 minor phase in the ternary blend. In other words, in compatibilized ternary blends the terminal relaxation time (interfacial relaxation) is contributed by the interfacial interactions between both the EPDM and PA6 minor components with the PP matrix, whereas in the uncompatibilized ternary blends the interfacial relaxation is primarily due to the interface between the EPDM phase and the matrix. The relaxation data of binary blends of PP/EPDM and PP/PA indicated that the relaxation time of the dispersed PA particles is higher than that of EPDM particles (Fig. 5a). Therefore in the relaxation spectrum of the ternary system, the different particles should relax in different times. However, the results show that the relaxation peaks of different dispersed particles convolute with each other to form a single relaxation peak, due to the nearness of the relaxation time scales. Nonetheless, the results clearly show that the relaxation peak of ternary system shifts to lower relaxation times with increasing the EPDM content, showing the increased contribution of EPDM particles.

FT-IR analysis

The FT-IR spectra for neat PP-*g*-MA and some of the binary and ternary blends are depicted in Fig. 6. The spectrum of PP-*g*-MA shows peaks at the range of 1713–1864 cm^{-1} most notably at 1787 cm^{-1} which is characteristic of cyclic anhydride groups. For binary and ternary blends containing PA6 phase, the peaks at 1515, 1630, 3017, 3178 and 3270 cm^{-1} are related to the different amine and/or amide linkages of the dispersed PA6 component. It can be seen that in the compatibilized PP/PA6 (70/30) and PP/PA6/EPDM (70/15/15) blends, the peak

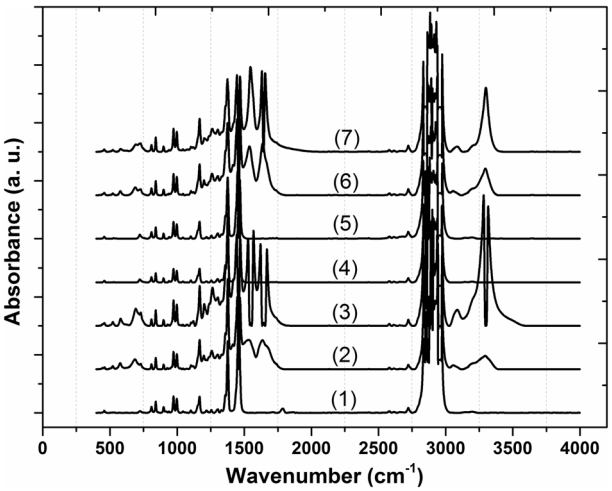

Fig. 6 FT-IR spectra for some of materials. *1* Neat PP-*g*-MA; *2* PP/PA6 (70/30); *3* PP/PA6/PP-*g*-MA (65/30/5); *4* PP/EPDM (70/30); *5* PP/EPDM/PP-*g*-MA (65/30/5); *6* PP/PA6/EPDM (70/15/15); *7* PP/PA6/EPDM/PP-*g*-MA (65/15/15/5)

related to the anhydride groups disappeared and/or shifted. The resulted imide linkage upon compatibilization is expected to show peaks at 1360 and 715 cm^{-1} due to the C–N– in the cyclic imide. It seems that these peaks overlapped with the characteristic peaks of other chemical bonds of the blend components. Compatibilization is considered to occur through chemical linkage of anhydride on the PP-*g*-MA chain and the PA6 end groups. This was evidenced by rheological measurements and can be further confirmed by SEM observations. Moreover, both PP/EPDM and PP/EPDM/PP-*g*-MA samples exhibit similar FT-IR spectra, indicating that no significant chemical bonding occurred in PP/EPDM modified by PP-*g*-MA. This finding is in accordance with the rheological results presented earlier.

Theoretical prediction of phase morphology in PP/EPDM/PA6 ternary blends

It has well been documented that the morphology of ternary blends can be predicted through the knowing of interfacial tension values between the components [40–44]. Hobbs et al. [41] used the spreading coefficient concept and rewrote Harkin's equation to predict the morphology of ternary blends, in which two distinct minor phases are dispersed in a major matrix phase. In a ternary blend of three polymers A, B and C (A is the matrix), the spreading coefficient, λ_{CB}, is defined as:

$$\lambda_{CB} = \gamma_{BA} - \gamma_{CA} - \gamma_{BC} \quad (1)$$

where λ_{ij} is the spreading coefficient of *i* component over *j* component and γ_{ij} is the interfacial tension between *i* and *j* components. For B to be encapsulated by C, λ_{CB}

Table 1 The surface tension data for PP, PA6 and EPDM calculated at 230 °C

Polymer	γ (mN/m)	γ^{p} (mN/m)	γ^{d} (mN/m)	dγ/dT (mN/m °C)	References
PP	17.62	0.36	17.26	−0.056	[47]
PA6	38.37	13.92	24.45	−0.065	[47]
EPDM	21.14	0.17	20.97	–	–

Table 2 The interfacial tension values for polymer pairs at 230 °C

System	Interfacial tension, γ_{AB} (mN/m)
PP/PA6	14.10
PP/EPDM	0.43
PA6/EPDM	13.70

must be positive. In the case when both λ_{CB} and λ_{BC} are negative, B and C will tend to form separated phases in A phase.

In this work, the surface tensions of PP and PA6 were calculated on the basis of data reported for surface tensions at 260 °C, variation of surface tension with temperature (−dγ/dT) and polarities ($x_p = \gamma_p/\gamma$) [45]. Surface tension of EPDM was calculated by means of a simple mixture rule from surface tensions of PE, PP and polyethylidene norbornene (PENB). The surface tension of PENB was assumed to be the same as that for polybutadiene [46] because the ENB content in EPDM is low (approximately 4.5 wt%). Surface tension γ, dispersive contribution of γ (γ^{d}) and polar contribution of γ (γ^{p}) at 230 °C for all the used polymers are listed in Table 1.

Interfacial tension between polymers can be calculated from the well-known harmonic mean equation [45]:

$$\gamma_{AB} = \gamma_A + \gamma_B - \frac{4\gamma_A^d \gamma_B^d}{\gamma_A^d + \gamma_B^d} - \frac{4\gamma_A^p \gamma_B^p}{\gamma_A^p + \gamma_B^p} \quad (2)$$

The interfacial tension values at 230 °C calculated from the surface tension data are listed in Table 2.

The interfacial tension data demonstrate that in PP/PA6/EPDM ternary blend the interfacial tension values for PP/PA6 and PA6/EPDM are much higher than that of PP/EPDM. The insertion of interfacial tension values into Eq. (1) results in negative values for both λ_{CB} and λ_{BC} spreading coefficients (Table 3) by assuming that subscripts B and C are corresponding to the PA6- and EPDM-dispersed phases, respectively. This predicts that in the PP/EPDM/PA6 ternary blends of different dispersed phase compositions, neither of the dispersed components exhibits any tendency to spread over the other. In other words, the PA6 and EPDM minor components are separately distributed in the PP matrix.

Table 3 Spreading coefficient values for PP/PA6/EPDM ternary blends

Polymer pairs	Spreading coefficient, λ
PA6/EPDM	$\lambda_{BC} = -27.37$
EPDM/PA6	$\lambda_{CB} = -0.03$

A PP matrix, *B* PA6, *C* EPDM

Phase morphology

PP/PA6 binary blends

The SEM micrographs of cryogenically fractured cross-section surfaces of PP/PA6 (70/30) blend without and with 5 wt% of PP-*g*-MA are shown in Fig. 7.

For uncompatibilized PP/PA6 blend, the typical matrix/dispersed droplet-type morphology characteristic of immiscible binary blends is clearly visible. The broad particle size distribution of dispersed domains of PA6 phase and the sharp interface region between the phases are indicative of high interfacial tension between the components. There is also evidence of poor interfacial bonding in this system leading to PA6 particles being detached from the surrounding matrix material, leaving holes on the fracture surface under the fast cryogenic fracture or lying loose on the surface. Addition of PP-*g*-MA compatibilizer precursor with subsequent formation of PA-*g*-PP compatibilizer at the blend interface significantly changed the phase structure from heterogeneous system for uncompatibilized blend to homogeneous morphology for compatibilized one. The high magnification micrograph of compatibilized blend (Fig. 7d) represents that the PA6 particles are highly wetted and, therefore, completely embedded within the matrix material. As a result, it is difficult to distinguish the dispersed droplets from the matrix phase. This intimate mixing state arises from the strong interfacial adhesion between the matrix and dispersed phase. The morphological observations presented in Fig. 7 confirm the obtained results from dynamic viscoelastic studies of PP/PA6 blend described in previous sections.

PP/EPDM binary blends

Figure 8 depicts the SEM micrographs of cryogenically fractured cross-section surfaces of PP/EPDM blends without and with 5 wt% of PP-*g*-MA.

It should be noted that for visualizing the dispersion state of EPDM phase in the PP matrix, the EPDM was selectively extracted by cyclohexane prior to microscopic analysis of ternary and binary blends containing EPDM phase. The empty dark cavities visible on the fractured surfaces are the location of dispersed EPDM phase domains in the PP matrix. Due to the sufficient compatibility between EPDM rubbery phase and PP matrix, the SEM micrographs of unmodified PP/EPDM blend reveal that a fine and uniform dispersion of EPDM domains in the PP was achieved under the melt mixing process (Fig. 8a, b). Upon the addition of PP-*g*-MA, a little change was observed in the size of dispersed EPDM domains, representative of little effect of

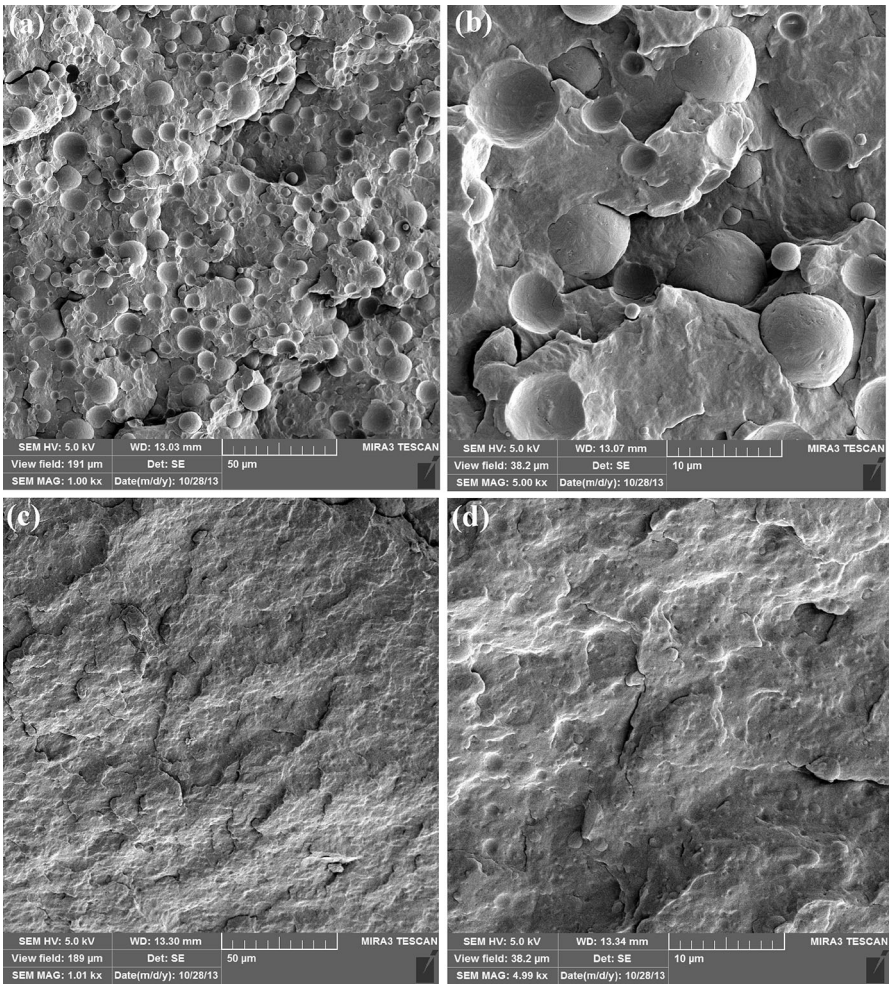

Fig. 7 SEM micrographs of **a**, **b** uncompatibilized and **c**, **d** compatibilized PP/PA6 (70/30) binary blends at different magnifications

PP-*g*-MA on the interfacial properties (Fig. 8c, d). The results of morphological observations for PP/EPDM blends described above are in agreement with those of rheological studies explained in previous sections, in that the PP-*g*-MA has a little effect on the dynamic viscoelastic properties of the PP/EPDM blends.

PP/EPDM/PA6 ternary blends

The SEM micrographs of cryogenically fractured cross-section surfaces of uncompatibilized and compatibilized PP/EPDM/PA6 ternary blends are shown in Figs. 9, 10 and 11.

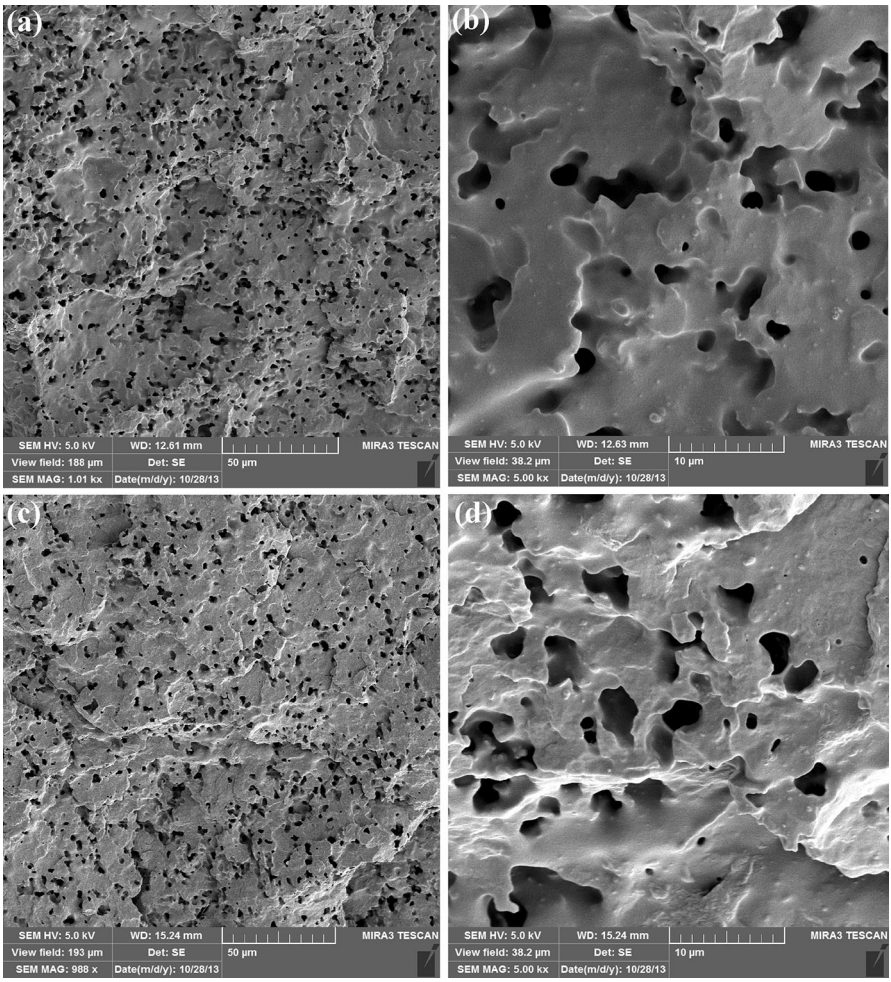

Fig. 8 SEM micrographs of **a**, **b** uncompatibilized and **c**, **d** compatibilized PP/EPDM (70/30) binary blends at different magnifications

In these micrographs, the tiny dark points visible on the fractured surfaces are the location of dispersed EPDM phase that has selectively been removed by solvent etching technique. The size of these particles is much smaller than that of PA6 particles in the uncompatibilized blends of different EPDM/PA6 weight ratios, which comes from the intrinsic compatibility of EPDM phase with PP matrix, contrary to the PA6 phase.

The micrographs reveal that the PA6 and EPDM phase domains are separately distributed within the PP matrix, with no interaction. This experimental observation is in good consistency with the theoretical prediction of phase morphology performed by spreading coefficient concept presented in previous section.

In the case of the dispersion state of EPDM phase in the matrix, it seems that increase in the concentration of rubbery phase from 15 to 20 wt% caused certain

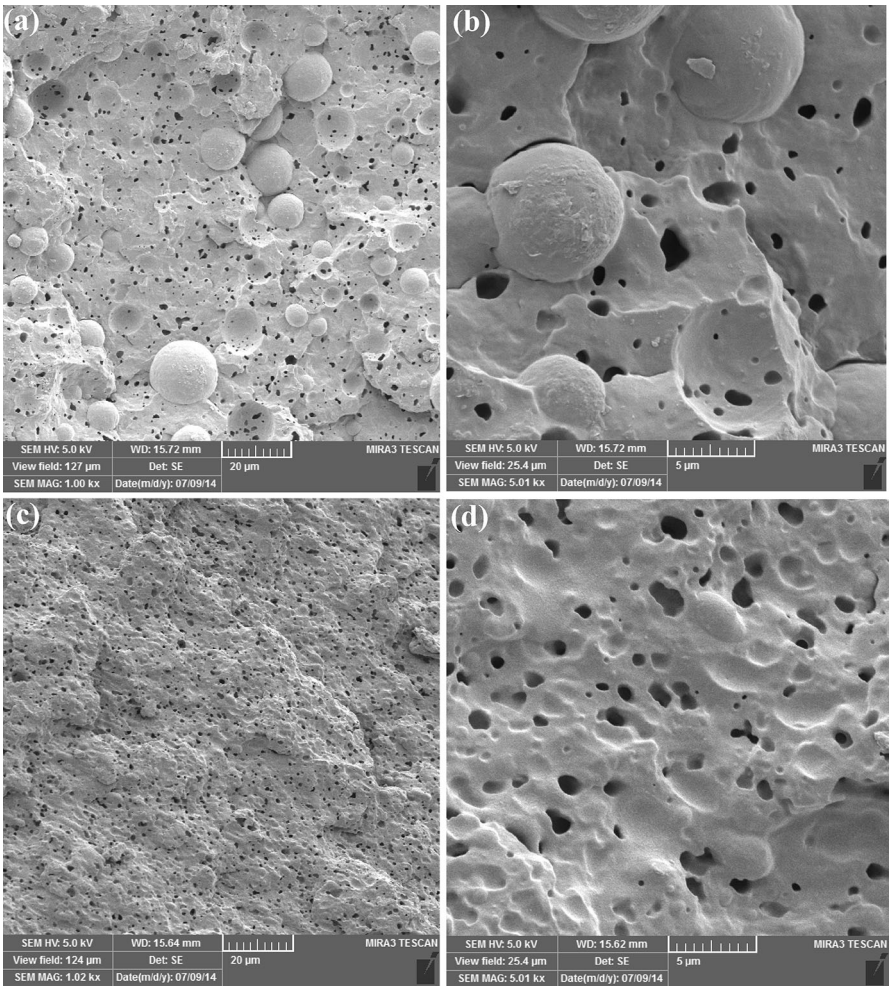

Fig. 9 SEM micrographs of **a**, **b** uncompatibilized and **c**, **d** compatibilized PP/EPDM/PA6 (70/10/20) ternary blend at different magnifications

particle percolation in the matrix, leading to the formation of larger irregularly shaped dispersed domains of EPDM phase in the ternary system. Therefore, it can be concluded that a change in morphological texture of EPDM domains from discrete semi-spherical particles into larger percolated domains having irregular shape is responsible for a substantial change observed in rheological properties, where a transition from liquid-like behavior to semi-solid-like behavior was observed with increasing the EPDM content from 15 to 20 wt% (Fig. 4). This confirms the reliability of rheological properties and their sensitivity in evaluation of morphology and morphology changes.

Similar to binary PP/PA6 blend, the incorporation of PP-*g*-MA into ternary blends with different compositions led to a drastic change in phase structure of the

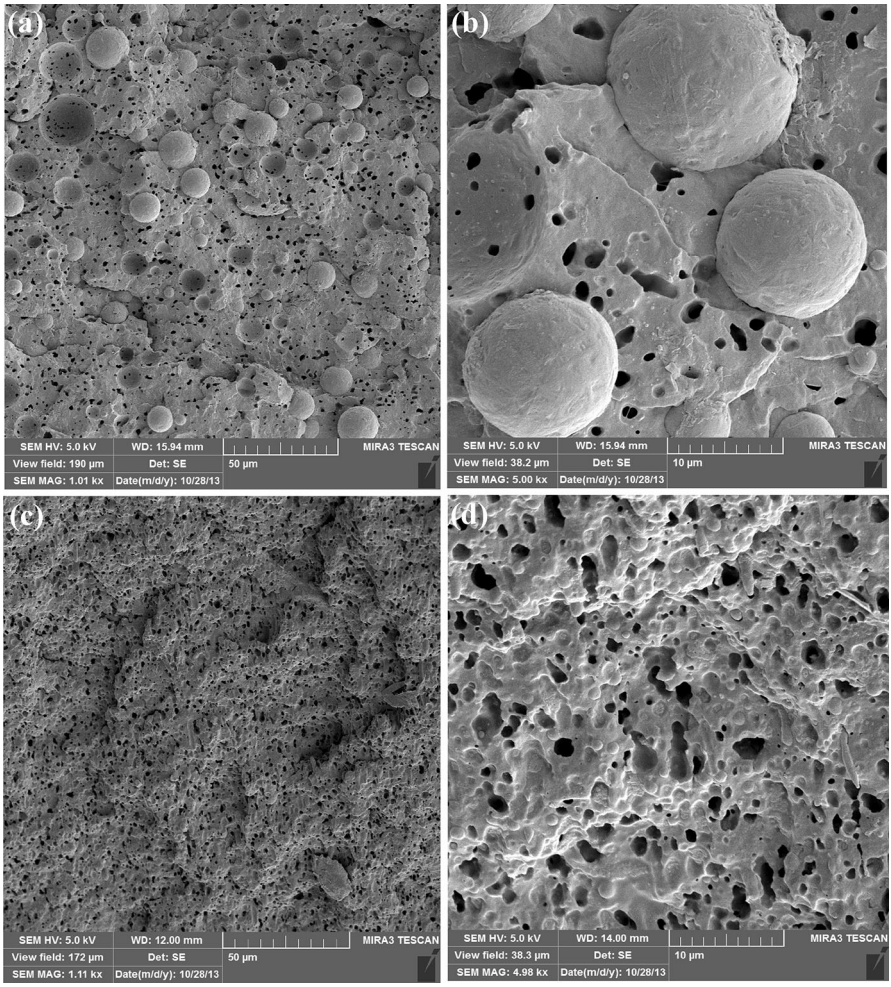

Fig. 10 SEM micrographs of **a**, **b** uncompatibilized and **c**, **d** compatibilized PP/EPDM/PA6 (70/15/15) ternary blend at different magnifications

blends. Compatibilization through the in situ formation of PP-*g*-PA6 copolymer during the mixing process greatly reduces the interfacial tension between the PA6 and PP phases which causes very fine dispersion of stabilized PA6 phase domains in the matrix, giving rise to the development of more homogeneous microstructure.

From Figs. 9, 10 and 11, it is reasonably clear that the average particle size of dispersed PA6 phase domains gradually decreased whereas that for EPDM rubbery phase was increased with progressive replacement of PA6 component by EPDM phase in the ternary blend. The normal distribution of approximate particle sizes for dispersed PA6 and EPDM components in the blends is given in Fig. 12.

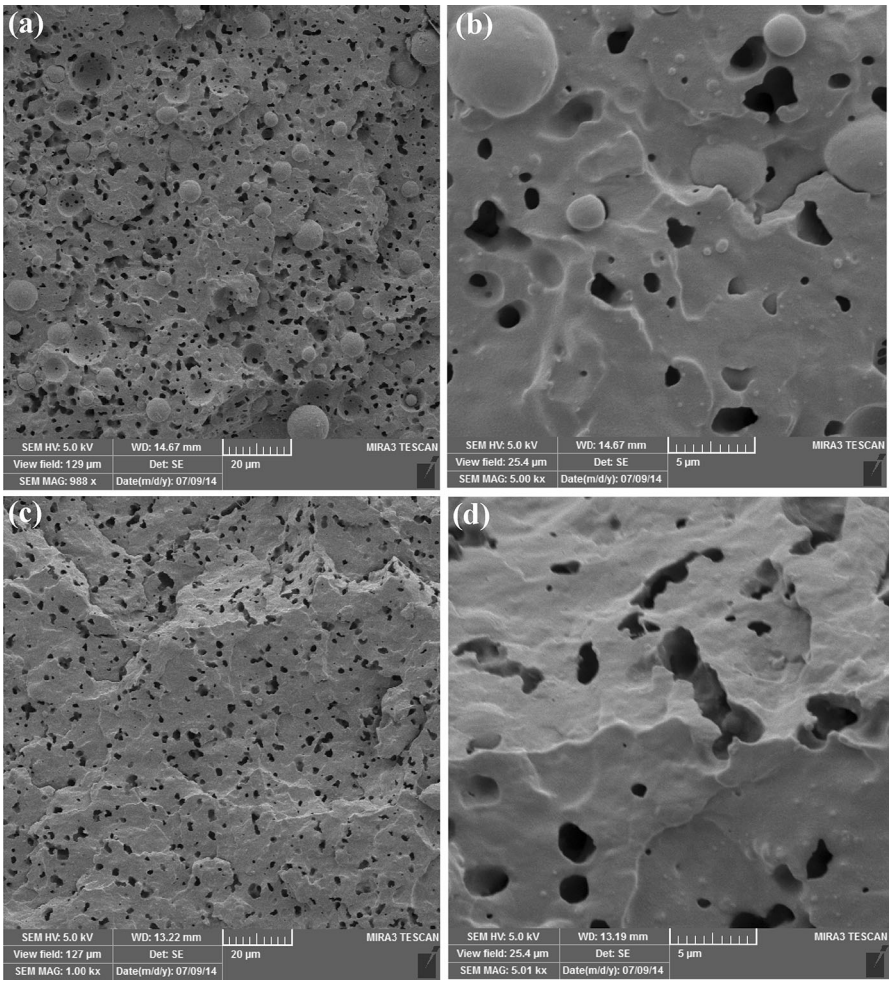

Fig. 11 SEM micrographs of **a**, **b** uncompatibilized and **c**, **d** compatibilized PP/EPDM/PA6 (70/20/10) ternary blend at different magnifications

Conclusions

The effects of blend composition and compatibilization process using PP-*g*-MA on the linear viscoelastic properties of binary and ternary blends of PP, PA6 and EPDM were investigated in connection with the blend morphologies. Obtained results led to the following conclusions:

- For PP/PA6 and PP/EPDM binary blends, the presence of 30 wt% of minor phase increased the melt viscosity and elasticity in conjunction with a decrease in the damping factor, especially at low frequencies. The extent of these changes in dynamic viscoelastic properties was much more pronounced for PP/EPDM

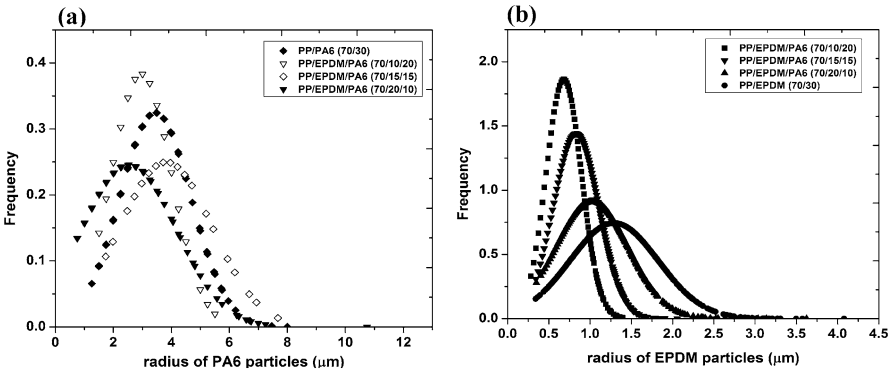

Fig. 12 Particle size distribution of dispersed components in different blends. **a** PA6 component, **b** EPDM component

binary blend, so that a remarkable deviation from liquid-like behavior was observed in this system. While PP-*g*-MA strongly changed the rheological properties of PP/PA6 binary blend, no clear effect was observed upon its incorporation into PP/EPDM binary blend. This finding was in accordance with the morphological observations made by SEM technique.

- In the case of PP/EPDM/PA6 ternary blends with 30 wt% of dispersed phase, the complex viscosity and melt elasticity gradually increased whereas the loss tangent decreased with the fraction of EPDM component in the blend. This was accompanied by a departure of rheological behavior into solid-like response. Compatibilization drastically changed the viscoelastic properties of ternary blends, with greater effect on the blends containing larger fraction of PA6 component. Compatibilized ternary blends exhibited higher viscosity and elasticity together with lower damping capacity than their uncompatibilized counterparts. Moreover, compatibilization extended the relaxation processes of blend systems toward prolonged relaxation times.
- The results of relaxation spectrum analysis revealed that the low-frequency response of different blend systems is controlled by the relaxation mechanisms related to the shape of dispersed droplets and/or interfacial region between the components and the matrix. In the uncompatibilized ternary blends, the interfacial relaxation was attributed to the interface region between the EPDM particles and matrix phase, whereas in compatibilized ternary blends the interface regions between both the PA6- and EPDM-dispersed components and the matrix concurrently contribute in the relaxation behavior of the blend. This was responsible for highly elastic behavior of compatibilized blends at low frequencies which is the characteristic of materials with solid-like response.

References

1. Utracki LA (1990) Polymer alloys and blends: thermodynamics and rheology. Hanser, Munuch

2. Han CD (1981) Multiphase flow in polymer processing. Academic Press, New York
3. Li J, Favis BD (2001) Characterizing co-continuous high density polyethylene/polystyrene blend. Polymer 42:5047
4. Kim TY, Kim DM, Kim WJ, Lee TH, Suh KS (2004) Effects of poly[styrene-b-(ethylene-cobutylene)-b-styrene] on the charge distributions of low-density polyethylene/polystyrene blends. J Polym Sci B Polym Phys 42:2813
5. Macaubas PHP, Demarquette NR (2001) Morphologies and interfacial tensions of immiscible polypropylene/polystyrene blends modified with triblock copolymers. Polymer 42:2543–2554
6. Bonner JG, Hope PS (1993) In: Folkes MJ, Hope PS (eds) Polymer blends and alloys, chap 3. Blackie, London, pp 46–75
7. Utracki LA (1995) History of commercial polymer alloys and blends (from a perspective of the patent literature). Polym Eng Sci 35(1):2–17
8. Van Hemelrijck E, Van Puyvelde P, Velankar S, Macosko CW, Moldenaers P (2004) Interfacial elasticity and coalescence suppression in compatibilized polymer blends. J Rheol 48:143–159
9. Van Hemelrijck E, Van Puyvelde P, Velankar S, Macosko CW, Moldenaers P (2005) The effect of block copolymer architecture on the coalescence and interfacial elasticity in compatibilized polymer blends. J Rheol 49:783–798
10. Ide F, Hasegawa A (1974) Studies on polymer blend of nylon 6 and polypropylene or nylon 6 and polystyrene using the reaction of polymer. J Appl Polym Sci 18:963
11. Scholz P, Froelich D, Muller R (1989) viscoelastic properties and morphology of two phase polypropylene/polyamide 6 blends in the melt. Interpretation of results with an emulsion model. J Rheol 33:481
12. Park SJ, Kim BK, Jeong HM (1990) Morphological, thermal and rheological properties of the blends polypropylene/nylon-6, polypropylene/nylon-6/(maleic anhydride-g-polypropylene) and (maleic anhydride-g-polypropylene)/nylon-6. Eur Polym J 26:131
13. Tedesco A, Barbosa RV, Nachtigall SMB, Mauler RS (2002) Comparative study of PP-MA and PP-GMA as compatibilizing agents on polypropylene/nylon 6 blends. Polym Testing 21:11–15
14. Rosch J, Mulhaupt R (1995) Mechanical and morphological properties of elastomer-modified polypropylene/polyamide-6 blends. J Appl Polym Sci 56:1599–1605
15. Gonzalez-Montiel A, Keskkula H, Paul DR (1995) Impact-modified nylon-6 polypropylene blends. 1. Morphology–property relationships. Polymer 36(24):4587–4603
16. Gonzalez-Montiel A, Keskkula H, Paul DR (1995) Impact-modified nylon 6/polypropylene blends: 2. Effect of reactive functionality on morphology and mechanical properties. Polymer 36(24):4605–4620
17. Ohlsson B, Hassander H, Tornell B (1998) Improved compatibility between polyamide and polypropylene by the use of maleic anhydride grafted SEBS. Polymer 39(26):6705–6714
18. Wong SC, Mai YW (1999) Effect of rubber functionality on microstructures and fracture toughness of impact-modified nylon 6,6/polypropylene blends: 1. Structure–property relationships. Polymer 40:1553–1566
19. Wilkinson AN, Laugel L, Clemens ML, Harding VM, Marin M (1999) Phase structure in polypropylene/PA6/SEBS blends. Polymer 40:4971–4975
20. Ou Y, Lei Y, Fang X, Yang G (2004) Maleic anhydride grafted thermoplastic elastomer as an interfacial modifier for polypropylene/polyamide 6 blends. J Appl Polym Sci 91:1806–1815
21. Wilkinson AN, Clemens ML, Harding VM (2004) The effects of SEBS-g-maleic anhydride reaction on the morphology and properties of polypropylene/PA6/SEBS ternary blends. Polymer 45:5239–5249
22. Baia SL, Wang GT, Hiver JM, G'Sell C (2004) Microstructures and mechanical properties of polypropylene/polyamide 6/polyethelene–octene elastomer blends. Polymer 45:3063–3071
23. Krache R, Benachour D, Potschke P (2004) Binary and ternary blends of polyethylene, polypropylene, and polyamide 6,6: the effect of compatibilization on the morphology and rheology. J Appl Polym Sci 94:1976–1985
24. Li Y, Wang D, Zhang JM, Xie XM (2011) Compatibilization and toughening of immiscible ternary blends of polyamide 6, polypropylene (or a propylene–ethylene copolymer), and polystyrene. J Appl Polym Sci 119:1652–1658
25. Yang H, Wang BK, Sun T, Wang X, Zhang Q, Fu Q, Dong X, Han CC (2008) Rheology and phase structure of PP/EPDM/SiO2 ternary composites. Eur Polym J 44:113–123
26. Su FH, Huang HX (2009) Mechanical and rheological properties of PP/SEBS/OMMT ternary composites. J Appl Polym Sci 112:3016–3023

27. Marcilla A, Garcia-Quesada JC, Lopez M, Gil E (2009) Study of the behavior of blends of a poly(hydroxybutyrate-valerate) copolymer, polypropylene, and SEBS. J Appl Polym Sci 113:3187–3195
28. Mostofi N, Nazockdast H, Mohammadigoushki H (2009) Study on morphology and viscoelastic properties of PP/PET/SEBS ternary blend and their fibers. J Appl Polym Sci 114:3737–3743
29. Basseri G, Mehrabi Mazidi M, Hosseini F, Razavi Aghjeh MK (2014) Relationship among microstructure, linear viscoelastic behavior and mechanical properties of SBS triblockcopolymer compatibilized PP/SAN blend. Polym Bull 71:465–486
30. Favis BD, Willis JM (1990) Phase size/composition dependence in immiscible blends: experimental and theoretical considerations. J Polym Sci B Polym Phys 28:2259–2269
31. Bureau MN, Elkadi H, Denault J, Dickson JI (1997) Injection and compression molding of polystyrene/high-density polyethylene blends—phase morphology and tensile behavior. Polym Eng Sci 37:377
32. Dai S, Ye L, Hu G (2010) Preparation and properties of PP/PC/POE blends. Polym Adv Technol 21:279–289
33. Xue CH, Wang D, Xiang B, Chiou B-S, Sun G (2011) Morphological development of polypropylene in immiscible blends with cellulose acetate butyrate. J Polym Res 18:1947–1953
34. Zheng Q, Zhang XW, Pan Y, Yi XS (2002) Polystyrene/Sn–Pb alloy blends. I. Dynamic rheological behavior. J Appl Polym Sci 86:3166
35. Wu D, Zhang Y, Zhang M, Zhou W (2008) Phase behavior and its viscoelastic responses of PLA/PCL blend. Eur Polym J 44:2171–2183
36. Ezzati P, Ghasemi I, Karrabi M, Azizi H (2008) Rheological behaviour of PP/EPDM blend: the effect of compatibilization. Iran Polym J 17:265–272
37. GuoZ Tong L, Fang Z (2005) In situ compatibilization of polystyrene/polyolefin elastomer blends by the Friedel–Crafts alkylation reaction. Polym Int 54:1647–1652
38. Riemann RE, Cantow HJ, Friedrich C (1996) Rheological investigation of form relaxation and interface relaxation processes in polymer blends. Polym Bull 36:637–643
39. Riemann RE, Cantow HJ, Friedrich C (1997) Interpretation of a new interface-governed relaxation process in compatibilized polymer blends. Macromolecules 30:5476–5484
40. Guo HF, Packirisamy S, Gvozdic NV, Meier DJ (1997) Prediction and manipulation of the phase morphologies of multiphase polymer blends: 1. Ternary systems. Polymer 38:785–794
41. Hobbs SY, Dekkers MEJ, Watkins VH (1988) Effect of interfacial forces on polymer blend morphologies. Polymer 29:1598–1602
42. Reignier J, Favis BD (2000) Control of the subinclusion microstructure in HDPE/PS/PMMA ternary blends. Macromolecules 33:6998–7008
43. Reignier J, Favis BD, Heuzey MC (2003) Factors influencing encapsulation behavior in composite droplet-type polymer blends. Polymer 44:49–59
44. Valera TS, Morita AT, Demarquette NR (2006) Study of morphologies of PMMA/PP/PS ternary blends. Macromolecules 39:2663–2675
45. Wu S (1982) Polymer interface and adhesion. Marcel Dekker, New York
46. Luzinov I, Pagnoulle C, Xi K, Huynh-Ba G, Jerome R (1999) Composition effect on the core–shell morphology and mechanical properties of ternary polystyrene/styrene–butadiene rubber/polyethylene blends. Polymer 40:2511
47. Omonov TS, Harrats C, Groeninckx G (2005) Co-continuous and encapsulated three phase morphologies in uncompatibilized and reactively compatibilized polyamide 6/polypropylene/polystyrene ternary blends using two reactive precursors. Polymer 46:12322–12336